Relaxation of a field-unwound cholesteric liquid crystal

I-An Yao, Yin-Chieh Lai, and Shu-Hsia Chen
Institute of Electro-Optical Engineering, National Chiao Tung University, Hsinchu 300, Taiwan, Republic of China

Jin-Jei Wu
Department of Electro-Optical Engineering, National Taipei University of Technology, Taipei 106, Taiwan, Republic of China
(Received 26 April 2004; published 22 November 2004)

We have numerically investigated the homogeneous-planar and homeotropic-planar transitions, respectively, in a planar-aligned cholesteric liquid crystal by using our multidimensional software based on the finite element method. When the unwinding field is turned off abruptly, the relaxation process of a field-unwound cholesteric liquid crystal is accompanied by an elastic-induced Helfrich deformation without introduction of defects, which will continuously convert into a stable planar texture with natural pitch and domain wall.

DOI: 10.1103/PhysRevE.70.051705 PACS number(s): 64.70.Md, 78.20.Bh, 46.15.−x

I. INTRODUCTION

A cholesteric liquid crystal (ChLC) possesses a periodic helical structure due to the chirality of molecules. In a ChLC with a positive dielectric anisotropy ($\Delta\varepsilon > 0$), a field-induced cholesteric-nematic phase transition was theoretically predicted [1] and experimentally observed [2]. When the electric field is applied perpendicular to the helical axis of a ChLC with a planar texture, a stepwise change in the pitch with an increase in the field is theoretically predicted [3] and experimentally observed [4]. At sufficiently strong field strength, the field-induced homogeneous state is obtained [1,5], as shown in Fig. 1. The critical field is given by $E_c = (\pi^2/P_0)(K_{22}/\Delta\varepsilon\varepsilon_0)^{1/2}$ where P_0 is the natural pitch of a ChLC and K_{22} is the twist elastic constant [1].

On the other hand, when the electric field is applied parallel to the helical axis, the ChLC layers may undergo sinusoidal periodic modulation under the application of a weak electric field. The modulation results from the frustration caused by the competition between the chirality, which favors a twist deformation, and the electric field, which favors alignment of molecules parallel to the field. The threshold field and period of the sinusoidal periodic deformation were first theoretically described by Helfrich [6] and refined by Hurault [7] and Chigrinov [8], respectively. On increasing the electric field, a 90° rotation of the helical axis occurs and the fingerprint (or focal conic) state forms. After the fingerprint state is formed, the untwisting process of the helix with increase of the electric field is similar to the cholesteric-homogeneous transition and the field-induced homeotropic state is obtained [5], as shown in Fig. 1.

When the external field is turned off abruptly, the relaxation process from the field-induced homogeneous or homeotropic state to the stable planar state is frustrated and then will be accompanied by a Helfrich-like periodic modulation. This modulation is due to the frustration caused by the competition of chirality, which favors a twist deformation, and boundary constraints, which favor the alignment of molecules parallel to the surfaces. Similar Helfrich-like periodic deformations have been experimentally observed in a planar-aligned ChLC by mechanically untwisting the helix or by a temperature-induced pitch variation [9]. However, the mechanisms of the periodic pattern formations and the detailed transformation processes were not presented. One can classify these Helfrich-like deformations into two types according to the driving sources for the deformations [10,11]. One is the field-induced Helfrich deformation. The other is the elastic-induced Helfrich deformation. In the former case, the ChLC layers form the sinusoidal deformation to alleviate the dielectric free energy of the system. However, for the latter case, the ChLC layers from the sinusoidal deformation in order to reduce the elastic free energy of the system.

In this paper, we will numerically investigate the dynamic relaxation process from the field-induced homogeneous and homeotropic states, respectively, to a stable planar state and show the transformation between states. The transformation

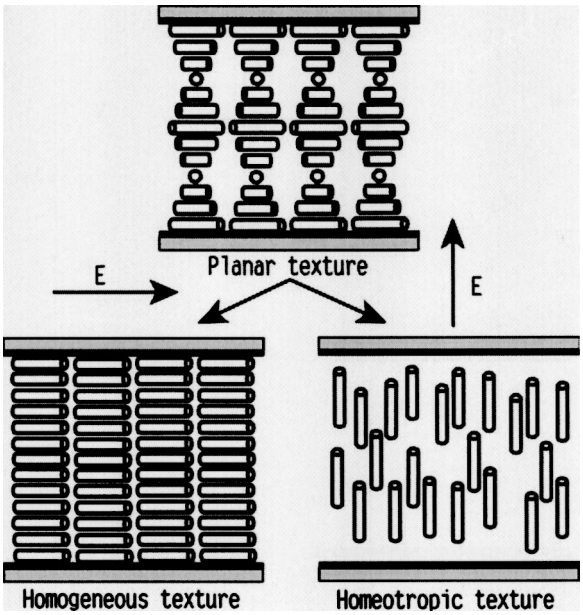

FIG. 1. Schematic diagram of a field-unwound cholesteric liquid crystal. If the electric field is applied perpendicular to the helical axis, the field-induced homogeneous state is obtained. If the electric field is applied parallel to the helical axis, the field-induced homeotropic state is obtained.

is an elastic-induced Helfrich deformation. We find that the relaxation process of a field-unwound ChLC occurs via an elastic-induced Helfrich deformation without introduction of defect cores.

II. SIMULATION METHOD

The simulation method is based on a variational approach to the Frank-Oseen free energy formulation and using a vectorial representation of the director. The modeling uses a finite element method for calculations of the director configuration and voltage distribution while it uses the finite difference method in the time stepping process [12].

The expression for the elastic free energy F_b of a ChLC system in terms of the director $\vec{n}$ is given by

$$F_b = \frac{1}{2}\int\int\int [K_{11}(\vec{\nabla}\cdot\vec{n})^2 + K_{22}(\vec{n}\cdot\vec{\nabla}\times\vec{n})^2 + K_{33}(\vec{n}\times\vec{\nabla}\times\vec{n})^2 + 2K_{22}q_0(\vec{n}\cdot\vec{\nabla}\times\vec{n})]dx\,dy\,dz, \quad (1)$$

where K_{11}, K_{22}, and K_{33} are the elastic constants for splay, twist, and bend deformations, respectively. $q_0(=2\pi/P_0)$ is the chiral parameter. The expression for the electric free energy F_e of a liquid crystal system in terms of the voltage v is given by

$$F_e = \frac{1}{2}\int\int\int \{\varepsilon_0\varepsilon_\perp(-\vec{\nabla}v)^2 + \varepsilon_0\Delta\varepsilon[\vec{n}\cdot(-\vec{\nabla}v)]^2\}dx\,dy\,dz, \quad (2)$$

where the dielectric anisotropy $\Delta\varepsilon=\varepsilon_\parallel-\varepsilon_\perp$ and $\varepsilon_\parallel, \varepsilon_\perp$ are the parallel and perpendicular permittivities of the director relative to the electric field.

Based on the finite element method, the director and voltage within an element can be expressed in terms of the nodal director and nodal voltage, respectively, as well as the interpolation function; therefore, we have

$$\vec{n} = \sum_{i=1}^{4} S_i(x,y,z)\vec{n}^i,$$

$$v = \sum_{i=1}^{4} S_i(x,y,z)v^i. \quad (3)$$

Here $S_i(x,y,z)$ is the interpolation function, $\vec{n}^i$ is the nodal director at node i, and v^i is the nodal voltage at node i. By substitution of Eq. (3) into Eqs. (1) and (2), the Gibbs free energy in Eq. (4) for one element can be expressed in terms of the nodal director and nodal voltage of the element:

$$F_g = F_b - F_e. \quad (4)$$

Ignoring the flow of the director, the dynamic equation of the director becomes a nonlinear equation for the nodal director component as expressed by [13,14]

$$\frac{\partial F_g}{\partial n_\delta^p} - \frac{\partial}{\partial n_\delta^p}\left(\frac{\lambda}{2}\int\int\int n_\mu^p n_\mu^p dx\,dy\,dz\right) + \frac{\partial}{\partial \dot{n}_\delta^p}\left(\frac{\gamma}{2}\int\int\int \dot{n}_\mu^p \dot{n}_\mu^p dx\,dy\,dz\right) = 0, \quad (5)$$

where the Lagrange multiplier λ is used to maintain the unit length of the director and the integrations are performed over the volume of a tetrahedral element. However, one cannot simultaneously solve this equation for λ and $\vec{n}$. Therefore, the λ term is dropped and $\vec{n}$ is renormalized to have a unit length after each time step [15,16]. In each element, for $\delta=x$, y, or z, $p=1$, 2, 3, or 4, and μ $(=x, y,$ and $z)$ implies summation, where γ is the rotational viscosity of a liquid crystal material. After using the forward difference approximation for the time derivative, we can obtain the numerical update equation for the director at each node in terms of the directors and voltage at that and surrounding nodes. Given the initial conditions for directors and voltage, this update equation for the nodal director can be solved by the relaxation method which is stable and gives acceptable convergence [16].

Because the dielectric constant is anisotropic, the voltage at each node depends on the directors at that and surrounding nodes. After solving Maxwell's equation in Eq. (6), a linear equation for the nodal voltage is derived:

$$\vec{\nabla}\cdot\vec{D} = 0, \quad (6)$$

where $\vec{D}$ is the electric displacement. Given a director configuration, this equation can be rewritten as a numerical update equation for voltage at current node in terms of the neighboring nodal voltage and it can be directly solved using the successive over-relaxation method [16].

In order to calculate the dynamics of the system, the new director configuration must be calculated before any variables are updated. When the old director configuration is updated by the new director configuration after each time step, the voltage distribution can be calculated directly or iterated to converge to the equilibrium distribution because the redistribution of the voltage with the director orientation is instantaneous.

In this simulation, we use periodic boundary conditions in the X and Y directions. Dirichlet boundary conditions are assumed for the planes $Z=0$, $Z=d$ corresponding to strong anchoring. If the applied electric field is larger than E_c, the director at each node in the bulk can be initially assumed to be (1,0,0) and (0,0,1) for the field-induced homogeneous and homeotropic states, respectively. When the electric field is turned off abruptly, some random noise is superposed on the initial bulk director configuration to avoid the system being in the metastable state. In the field-induced homogeneous state, we set n_y and n_z to random numbers between 0.1 and -0.1; then n_x can be determined based on the relationship $n_x=(1-n_y^2-n_z^2)^{1/2}$. On the other hand, in the field-induced homeotropic state, we set n_x and n_y to random numbers between 0.1 and -0.1; then n_z can be determined based on the relationship $n_z=(1-n_x^2-n_y^2)^{1/2}$. This random noise can be

thought to be thermal fluctuations and it affects the director configuration very little.

In this simulation, the following LC parameters (Merck ZLI-4792) are used: $K_{11}=13.2$ pN, $K_{22}=6.5$ pN, $K_{33}=18.3$ pN, $\Delta\varepsilon=5.2$ (at 1 kHz), $\varepsilon_{\perp}=3.1$, and $\gamma=0.133$ Pa s. The 3% chiral agent (Merck S811) is doped into the above host and this results in a natural pitch $P_0=2.98$ μm. The physical size of the cell in the calculation is assumed to be 6.4 and 6.4 μm in the X direction (rubbing direction) and Z direction (cell-normal direction), respectively, with 65×65 node points. Thus the thickness to pitch ratio (d/P_0) is 2.15. Fixed planar-aligned boundary conditions with a 4.0° pretilt angle are assumed.

III. RESULTS

In this section, we present our simulation results in the following manner. In Sec. III A, we present the relaxation process from the field-induced homogeneous state to a stable planar state. In Sec. III B, we present the relaxation process from the field-induced homeotropic state to the stable planar state. In each part, we will show the two-dimensional (X-Z plane) director configurations during the relaxation process of a field-unwound ChLC. In these figures, the director at each node of the element is represented as a cylindrical rod. The orientation of the cylindrical rod indicates the average orientation of ChLC molecules at the point in space associated with that node. For a clear view, these figures are drawn sampled.

A. Homogeneous-planar relaxation

The planar-aligned ChLC can be unwound to a homogeneous state, as shown in Fig. 2(a), when the electric field is applied perpendicular to the helical axis and the field strength is larger than E_c. We will define the time $t=0$ as the time at which the voltage is removed. Because the chiral parameter is not equal to zero, i.e., $q_0\neq0$, the ChLC molecules incline to twist to the planar state. However, the boundary constraints hinder the twist deformation. Under the competition of chirality and boundary constraints, the molecules are seen to form the sinusoidal Helfrich deformation to alleviate the stored high twist energy, as shown in Fig. 2(b). Moreover, the wavelength of the Helfrich deformation roughly equals the theoretical value derived by Chigrinov *et al.*, which is induced by the external field [8]. The period is given as

$$\lambda=[P_0 d(3K_{33}/2K_{22})^{1/2}]^{1/2}, \tag{7}$$

where d is the cell gap. Considering the parameters used in the simulation, one gets $\lambda=6.26$ μm. As expected, there is one full wavelength in the X direction, as shown in Fig 2(b). Furthermore, the direction of Helfrich deformation is parallel to the director orientation in the middle layer of the cell. Therefore, one will observe a stripe with direction perpendicular to the rubbing direction and this result agrees well with the previous experimental observation [4]. As can be seen in Fig. 2(c), the amplitude of the modulation increases with time and the twist deformation in the bulk occurs. Here,

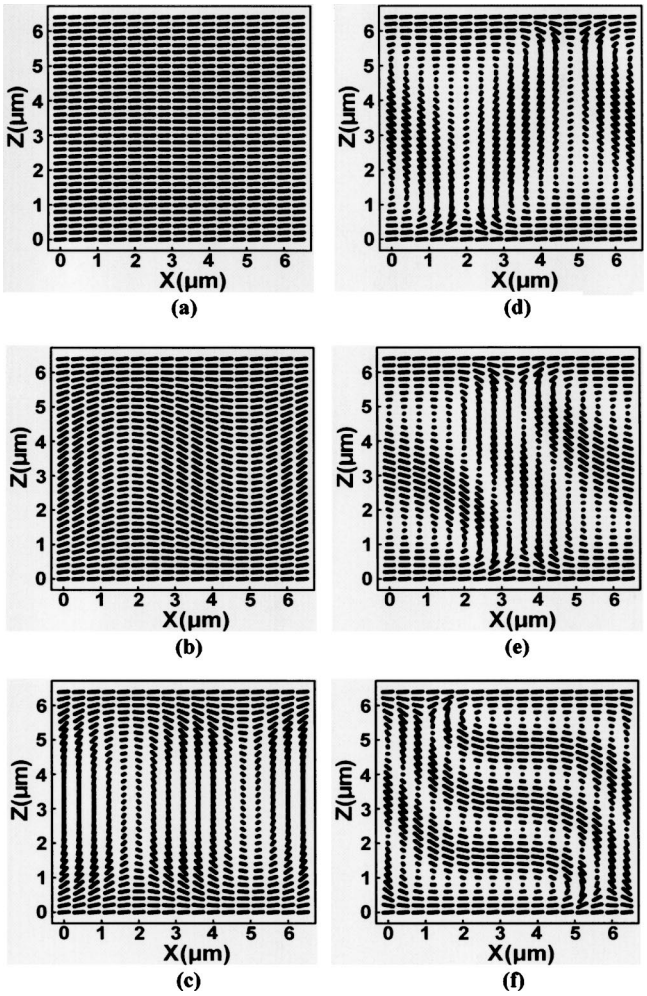

FIG. 2. Simulated director configurations during the relaxation from the field-induced homogeneous state to the planar state. Times are (a) 0.2 ms, (b) 100 ms, (c) 110 ms, (d) 250 ms, (e) 700 ms, and (f) 1500 ms.

the modulation no longer exhibits a sinusoidal appearance, but rather appears to exhibit fingers that grow from the surfaces in a spatially alternating fashion. As time progresses, the ends of the fingers spread out horizontally and overlap each other, as shown in Fig. 2(d). In this stage, the ChLC possesses a nonequilibrium pitch length; hence, the layers proceed to distort and overlap each other to increase the number of pitches, as shown in Fig. 2(e). This results in the formation of an equilibrium region with intrinsic pitch and domain wall that separates the stable planar texture, as shown in Fig. 2(f). As expected, the equilibrium region has two full 360° twists ($d/P_0=2.15$).

The model obtained agrees well with the previous experimental observation that for an abrupt turn-off of the relaxation of a field-unwound ChLC is accompanied by the appearance of spatially modulated texture and this texture will then gradually convert into a stable planar texture with a domain wall [4,17].

B. Homeotropic-planar relaxation

For the comparison between the homogeneous-planar and homeotropic-planar transitions, we show a similar simulation

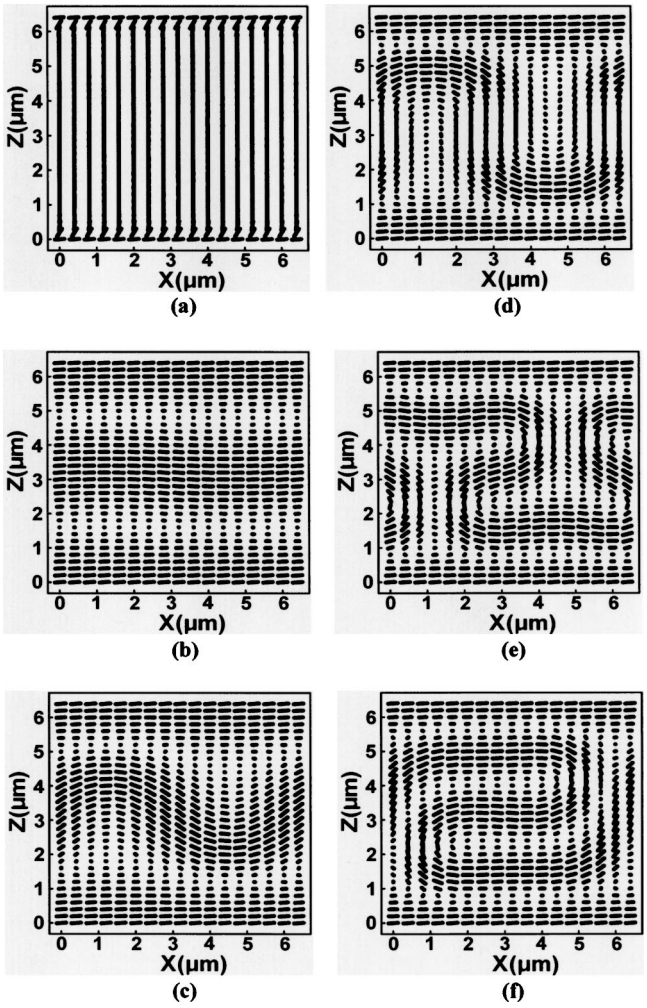

FIG. 3. Simulated director configurations during the relaxation from the field-induced homeotropic state to the planar state. Times are (a) 0.2 ms, (b) 365 ms, (c) 600 ms, (d) 765 ms, (e) 880 ms, and (f) 1300 ms.

to that presented in previous publications [11,12]. The initial state is a homeotropic state in which the natural twist has been completely removed through the application of an electric field parallel to the helical axis, as shown in Fig. 3(a). When the electric field is turned off from the homeotropic state, the ChLC molecules first go through a one-dimensional conical relaxation to the transient planar state, as shown in Fig. 3(b). The transient planar state is a metastable state with the effective pitch $P^* = (K_{33}/K_{22})P_0$ [18–20]. As expected, we have one full 360° twist in the transient planar state ($d/P^* = 0.76$). Due to the frustration caused by the competition between the chirality and boundary constraints, the ChLC molecules proceed through a Helfrich undulation, as shown in Fig. 3(c) during the transition from the transient planar state to a planar state. We find that the wavelength of the Helfrich undulation also matches well with the theoretical value in Eq. (7) and this has been experimentally confirmed [19]. As can be seen from Fig. 3(d), the modulation increases in amplitude as the simulation progresses and then the ends of the "fingers" mushroom out horizontally, as shown in Fig. 3(e). Figure 3(f) shows the equilibrium state with natural pitch and domain boundary. As expected, there are two full 360° twists in the equilibrium region ($d/P_0 = 2.15$).

IV. DISCUSSION

Figures 2 and 3 show the complete dynamic relaxation processes from the field-induced homogeneous and homeotropic states, respectively, to the stable planar state. From the viewpoint of the energy in the ChLC system, because the homogeneous state and transient planar state are all metastable states, the stored twist energy in these two states is higher than that in the ground state (planar state). This leads to instability of the system and the elastic-induced Helfrich deformation occurs in order to alleviate the high twist energy.

The random noise caused by thermal fluctuation of the director plays an important role for the occurrence of the Helfrich deformation. If this random fluctuation is not employed in the simulation, the ChLC molecules will relax to a metastable state and remain there. On the other hand, the formation process of the Helfrich deformation is a nucleation process. Therefore, it takes a long time to initiate the Helfrich deformation as shown in Figs. 2(a) and 2(b) and Figs. 3(b) and 3(c). However, the stored twist energy in the homogeneous state is higher than that in the transient planar state. Thus, the time to initiate the Helfrich deformation in the homogeneous state is shorter than that in the transient planar state.

V. CONCLUSIONS

The dynamic relaxation process of a field-unwound ChLC has been well described by our simulation. The relaxation from the field-induced homogeneous state to a stable planar state is in a sequence of homogeneous-planar transitions. However, the relaxation from the field-induced homeotropic state to a stable planar state is in a different sequence of homeotropic-transient planar-planar transitions. These relaxation processes occur via an elastic-induced Helfrich deformation without introduction of defects, which continuously converts into a stable planar texture with natural pitch and domain wall.

Based on our simulation results, we can conclude that an elastic-induced Helfrich deformation may be driven by the nonequilibrium layer spacing, induced either by external fields or mechanical strain fields or temperature variations, to increase the number of layers in a ChLC. In these situations, the structure of cholesteric layers favored by chirality can be achieved without the introduction of any defects.

ACKNOWLEDGMENTS

This work was partially supported by the National Science Council of the Republic of China under the Contracts No. NSC 92-2112-M-009-025 and No. NSC 92-2112-M-027-001.

[1] P. G. de Gennes, Solid State Commun. **6**, 163 (1968).
[2] R. B. Meyer, Appl. Phys. Lett. **12**, 281 (1968).
[3] R. Dreher, Solid State Commun. **13**, 1571 (1973).
[4] S. V. Belyaev and L. M. Blinov, JETP Lett. **30**, 99 (1979).
[5] M. Warner, E. M. Terentjev, R. B. Meyer, and Y. Mao, Phys. Rev. Lett. **85**, 2320 (2000).
[6] W. Helfrich, Appl. Phys. Lett. **17**, 531 (1970).
[7] J. P. Hurault, J. Chem. Phys. **59**, 2068 (1973).
[8] V. G. Chigrinov, V. V. Belyaev, S. V. Belyaev, and M. F. Grebenkin, Sov. Phys. JETP **50**, 994 (1979).
[9] C. J. Cerritsma and P. Van Zanten, Phys. Lett. **37A**, 47 (1971).
[10] P. G. Gennes and J. Prost, *The Physics of Liquid Crystals* (Oxford University Press, New York, 1993)
[11] P. Watson, J. E. Anderson, and P. J. Bos, Phys. Rev. E **62**, 3719 (2000).
[12] I. A. Yao, J. J. Wu, and S. H. Chen, Jpn. J. Appl. Phys., Part 1 **43**, 705 (2004).
[13] D. W. Berreman, Philos. Trans. R. Soc. London, Ser. A **309**, 203 (1983).
[14] D. W. Berreman, Appl. Phys. Lett. **25**, 12 (1974).
[15] S. Dickmann, J. Eschler, O. Cossalter, and D. A. Mlynski, SID Int. Symp. Digest Tech. Papers **24**, 638 (1993).
[16] H. Mori, E. C. Gartland, Jr., J. R. Kelly, and P. J. Bos, Jpn. J. Appl. Phys., Part 1 **38**, 135 (1999).
[17] E. Niggemann and H. Stegemeyer, Liq. Cryst. **5**, 739 (1989).
[18] M. Kawachi and O. Kogure, Jpn. J. Appl. Phys. **16**, 1673 (1977).
[19] P. Watson, J. E. Anderson, V. Sergan, and P. J. Bos, Liq. Cryst. **26**, 1307 (1999).
[20] D.-K. Yang and Z.-J. Lu, SID Int. Symp. Digest Tech. Papers **26**, 351 (1995).